aerodynamic forces than the imaginary part (although the benefits to the imaginary part are substantial in most cases).

There is sufficient benefit to the tip inset correction in all cases studied to make the recommendation that it be used routinely, particularly because the correction is so easily made. Only the case of equal width spanwise strips has been considered. Other spanwise distributions of strip width would require further investigation.

References

[1]Rubbert, P. E., "Theoretical Characteristics of Arbitrary Wings by a Non-Planar Vortex Lattice Method," The Boeing Co., D6-9244, Renton, WA, 1964.

[2]Hough, G. R., "Remarks on Vortex-Lattice Methods," *Journal of Aircraft*, Vol. 10, No. 5, 1973, pp. 314–317.

[3]Hough, G. R., "Lattice Arrangement for Rapid Convergence," *Vortex-Lattice Utilization*, NASA SP-405, May 1976, pp. 325–342.

[4]Rodden, W. P., Taylor, P. F., and McIntosh, S. C., Jr., "Further Refinement of the Nonplanar Aspects of the Subsonic Doublet-Lattice Lifting Surface Method," *Journal of Aircraft*, Vol. 35, No. 5, 1998, pp. 720–727.

[5]Rodden, W. P., Taylor, P. F., McIntosh, S. C., and Baker, M. L., "Further Convergence Studies of the Enhanced Subsonic Doublet-Lattice Oscillatory Lifting Surface Method," *Journal of Aircraft*, Vol. 36, No. 4, 1999, pp. 682–688.

[6]Baker, M. L., and Rodden, W. P., "Improving the Convergence of the Doublet-Lattice Method Through Tip Corrections," *International Forum of Aeroelasticity and Structural Dynamics*, Confederation of European Aerospace Societies, June 1999, pp. 763–775.

[7]Horsten, J. J., den Boer, R. G., and Zwaan, R. J., "Unsteady Transonic Pressure Measurements on a Semispan Wind Tunnel Model of a Transport-Type Supercritical Wing (LANN Model), Part I," Air Force Wright Aeronautical Lab., Rept. AFWAL-TR-83-3039, Dayton, OH, March 1983.

Parametric Study of the Phugoid

S. Pradeep*
Indian Institute of Science, Bangalore 560 012, India

Introduction

CONVENTIONAL aircraft exhibit both longitudinal and lateral-directional modes of motion because of the symmetry existing in their geometry, aerodynamics, and properties of the propulsive system. Longitudinal dynamics are comprised of the phugoid and the short period mode. Exact solutions to the phugoid and the short period modes are nonexistent. The literal approximation to the short period mode is well known[1] and represents a very faithful representation of reality. In contrast, the phugoid approximations developed by various authors have been unsatisfactory. On account of the inaccuracies in the phugoid approximation, it has not been possible to make accurate predictions of the effect of aerodynamic derivatives on the characteristics of the phugoid mode. Such a study is important because it can provide vital insights on the functional dependence of the modal parameters on the aerodynamic derivatives.

An approximation for the frequency and the damping of the phugoid mode was developed recently,[2,3] and it was shown to be a fair representation over a wide range of flight conditions for different types of aircraft. These literal expressions enable a meaningful parametric study. The literal expressions for the phugoid mode of a conventional aircraft are used to carry out a parametric study to bring out the effect of the aerodynamic derivatives, which is corroborated by numerical simulation over a broad spectrum database. The notations used in this paper are that of Roskam.[1] All of the thrust derivatives have been combined with the aerodynamic derivatives, i.e., X_u stands for $X_u + X_{T_u}$, M_u stands for $M_u + M_{T_u}$, and M_α stands for $M_\alpha + M_{T_\alpha}$.

Approximate Equations for the Phugoid

Many approximations to the phugoid with varying assumptions appear in literature.[3] Although excellent expressions have been derived for phugoid frequency, they have not received adequate exposure. On the other hand, none of the existing approximations for phugoid damping is worthy. Based on this finding, an approximate expression was derived[2,3] for ω_p and $2\zeta_p\omega_p$.

$$\omega_p = \sqrt{\frac{g\left(M_u Z_\alpha - M_\alpha Z_u\right)}{M_\alpha U_1 - Z_\alpha M_q}} \tag{1}$$

$$\begin{aligned} 2\zeta_p\omega_p = \frac{1}{M_\alpha U_1 - M_q Z_\alpha}\Bigg(& -g\sin\Theta_1 M_\alpha \\ & + X_u\left(g\sin\Theta_1 M_{\dot\alpha} - M_\alpha U_1 + M_q Z_\alpha\right) \\ & + Z_u\left\{-gM_{\dot\alpha} - M_q X_\alpha + \frac{gM_\alpha[U_1(M_{\dot\alpha} + M_q) + Z_\alpha]}{M_\alpha U_1 - M_q Z_\alpha}\right\} \\ & + M_u\left\{U_1(X_\alpha - g) - \frac{gZ_\alpha[U_1(M_{\dot\alpha} + M_q) + Z_\alpha]}{M_\alpha U_1 - M_q Z_\alpha}\right\}\Bigg) \end{aligned} \tag{2}$$

Numerical simulations involving 15 cases of various types of aircraft under varying flight conditions were carried out to verify the authenticity of this expression. These data of six modern aircraft in different flight conditions were taken from Appendix C of Roskam's text on flight dynamics.[1] The simulations confirmed that the difference between the approximate expression (1) and the exact value is less than 4% in the 15 cases considered.

Parametric Studies

The dependence of ω_p and ζ_p on individual aerodynamic derivatives is now investigated. The inquiries are based on the presumption that the stability derivatives can be changed one at a time, keeping all others fixed. The flight condition is also presumed to be held unchanged. The analytical expressions for ω_p and $2\zeta_p\omega_p$ were used to extract information wherever possible. At the same time numerical simulations were carried out over the same database by varying the derivatives over the range spanned by the variable and calculating the frequency and damping from the exact fourth-order characteristic equation. It is felt that the results obtained from such a provocative test involving so wide a variation of the aerodynamic derivatives is general enough for all practical purposes. Following the notation of Roskam,[1] the longitudinal characteristic equation is

$$As^4 + Bs^3 + Cs^2 + Ds + E = 0 \tag{3}$$

where

$$\begin{aligned} A &= U_1 - Z_{\dot\alpha} \\ B &= -(U_1 - Z_{\dot\alpha})(X_u + M_q) - Z_\alpha - M_{\dot\alpha}(U_1 + Z_q) \\ C &= X_u[M_q(U_1 - Z_{\dot\alpha}) + Z_\alpha + M_{\dot\alpha}(U_1 + Z_q)] \\ &\quad + M_q Z_\alpha - Z_u X_\alpha + M_{\dot\alpha} g\sin\Theta_1 - M_\alpha(U_1 + Z_q) \\ D &= g\sin\Theta_1(M_\alpha - M_{\dot\alpha}X_u) + g\cos\Theta_1[Z_u M_{\dot\alpha} + M_u(U_1 - Z_{\dot\alpha})] \\ &\quad - M_u X_\alpha(U_1 + Z_q) + Z_u X_\alpha M_q + X_u[M_\alpha(U_1 + Z_q) - M_q Z_\alpha] \\ E &= g\cos\Theta_1(M_\alpha Z_u - Z_\alpha M_u) + g\sin\Theta_1(M_u X_\alpha - X_u M_\alpha) \end{aligned} \tag{4}$$

It was seen from the simulation that only four derivatives have a significant effect on the frequency and damping. The variations in frequency and damping for these four derivatives are shown in Fig. 1.

Presented as Paper 00-0500 at the AIAA 38th Aerospace Sciences Meeting and Exhibit, Reno, NV, 10–13 January 2000; received 22 May 2000; revision received 21 January 2001; accepted for publication 5 February 2001.

*Associate Professor, Department of Aerospace Engineering. Member AIAA.

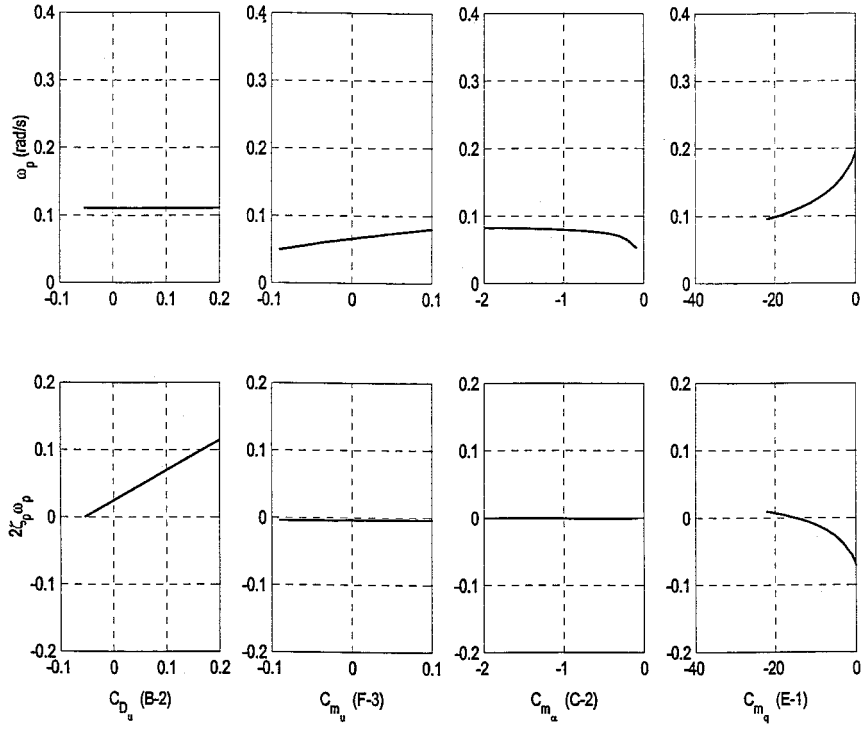

Fig. 1 Variation of phugoid frequency and damping with aerodynamic coefficients.

In the graphs the abscissa shows the aerodynamic derivative being varied, and the ordinate shows the frequency/damping. To facilitate comparison of results, uniformity is maintained in the graphs by ensuring that all of the ordinates vary from 0 to 0.4 for the frequency plots and from −0.2 to 0.2 in the damping plots. The abscissa of each graph is determined from the range spanned by the variable, obtained from the minimum and the maximum values in the database. The upper plots represent the variation in frequency, and the lower plots represent the damping. To conserve space, for each aerodynamic derivative, only one aircraft and flight condition, representing the largest variation in the 15 cases considered, is shown. The label on the x axis shows the aircraft and flight condition, in addition to the aerodynamic derivative being varied. The notation for the aircraft and the flight condition are taken from Appendix C of Roskam.[1] It consists of two symbols: a letter, followed by a number. The letter stands for the aircraft and the number for the flight condition. In the graphs shown in Fig. 1, B-2 represents a 19-passenger commuter airliner in low-altitude cruise; C-2, a small jet trainer in normal cruise; E-1, a supersonic fighter-bomber in power approach; and F-3, a large wide-body jet transport in low-altitude cruise.

The largest variation in C_{D_u} is seen for aircraft B in flight condition 2. The graph of ω_p vs C_{D_u}, which appears as the top left plot, and the graph of $2\zeta_p\omega_p$ vs C_{D_u}, which is the bottom left plot, are for the aircraft B in flight condition 2. Thus label for the extreme left plot shows B-2 in braces. Similarly, the largest variation in C_{m_q} is seen for aircraft E in flight condition 1. The graph of ω_p vs C_{m_q}, which appears as the top right plot and the graph of $2\zeta_p\omega_p$ vs C_{m_q}, which is the bottom right plot are for the aircraft E in flight condition 1. The label for the extreme right plot shows E-1 in braces.

Effect of Aerodynamic Derivatives on the Phugoid Frequency

From Eq. (1) it is seen at once that ω_p is dependent only on the derivatives Z_u, Z_α, M_u, M_α, and M_q. Before considering the influence of the aerodynamic derivatives, it is helpful to bear in mind their usual signs.

$$\omega_p^2 = \frac{\overset{(+)}{g}\ \overset{(\pm)}{(}\overset{(-)}{M_u Z_\alpha} - \overset{(-)}{M_\alpha} \overset{(-)}{Z_u})}{\underbrace{\overset{(-)}{M_\alpha}\overset{(+)}{U_1} - \overset{(-)}{Z_\alpha}\overset{(-)}{M_q}}_{(-)}}$$

When $M_u Z_\alpha - M_\alpha Z_u > 0$, ω_p becomes a complex number, and the approximation is rendered invalid. Also, observe that Z_u is negative in practice although C_{L_u} may be positive or negative.

The derivative of the phugoid frequency with respect to Z_u is given by

$$\frac{\partial \omega_p}{\partial Z_u} = \left(\frac{-gM_\alpha}{2\omega_p}\right)\frac{1}{(M_\alpha U_1 - Z_\alpha M_q)}$$

The first term on the right-hand side is positive in sign, and the second term is negative in sign, making the expression negative, implying that the phugoid frequency decreases with increase in Z_u. From the definition of C_{L_u} (Ref. 1), this is equivalent to saying that the phugoid frequency increases with increase in C_{L_u}. It is difficult to determine how significant the change is without recourse to airplane data. The numerical simulation shows that the change is not significant in the normal range of interest of C_{L_u} for most cases.

The derivative of the phugoid frequency with respect to Z_α is given by

$$\frac{\partial \omega_p}{\partial Z_\alpha} = \left(\frac{-gM_\alpha}{2\omega_p}\right)\frac{M_q Z_u - M_u U_1}{(M_\alpha U_1 - M_q Z_\alpha)^2}$$

The first term on the right-hand side is positive. The second term is positive if M_u is negative. If M_u is positive, the sign of the second term depends on the relative magnitudes of $M_u U_1$ and $M_q Z_u$, and no general conclusion can be drawn. The numerical simulation shows that when C_{L_α} increases sometimes ω_p increases and sometimes it decreases. In either case the change is too small to warrant attention. For all practical purposes it can be said that ω_p is invariant with respect to changes in Z_α.

When $M_u = M_\alpha Z_u / Z_\alpha$, the phugoid frequency vanishes. When M_u is less than this critical value, the phugoid mode is characterized by two first orders: one convergent and the other the divergent "tuck." The derivative of the frequency with respect to this derivative is given by

$$\frac{\partial \omega_p}{\partial M_u} = \left(\frac{-gZ_\alpha}{2\omega_p}\right)\frac{1}{(Z_\alpha M_q - M_\alpha U_1)}$$

Both terms on the right-hand side are positive, making $\partial\omega_p/\partial M_u > 0$. From the definition of C_{m_u} (Ref. 1), it can be said that

an increase in C_{m_u} results in an increase in ω_p and viceversa above the critical value of the derivative. Figure 1 shows the variation for aircraft F in flight condition 3.

The phugoid frequency remains almost invariant with C_{m_α} until it reaches a critical value $M_\alpha = M_u Z_\alpha / Z_u$, when it becomes zero.[4] At the critical value the phugoid frequency diverges with a slope of $-\infty$. When $M_q Z_\alpha / U_1 < M_u Z_\alpha / Z_u$, the divergence occurs earlier at $M_\alpha = M_q Z_\alpha / U_1$, and the slope of the curve suddenly changes to $+\infty$. Figure 1 shows the change for aircraft C in flight condition 2.

The derivative of ω_p with respect to C_{m_q} is given by

$$\frac{\partial \omega_p}{\partial M_q} = \frac{\omega_p \overbrace{Z_\alpha}^{(-)}}{2\underbrace{(M_\alpha U_1 - M_q Z_\alpha)}_{(-)}}$$

ω_p is thus directly proportional to M_q. From the definition of C_{m_q} (Ref. 1), it follows that ω_p is also directly proportional to C_{m_q}. Figure 1 depicts the variation for aircraft E in flight condition 1.

It has been shown[5] that in the speed range of interest of powered aircraft ω_p is invariant with respect to changes in the forward speed, dispelling the commonly held notion that the phugoid frequency is inversely proportional to the forward speed.

Effect of Aerodynamic Derivatives on the Phugoid Damping

Unlike the frequency equation, the approximation to damping [Eq. (2)] is comparatively more complicated. All derivatives except C_{D_q}, C_{L_q}, and $C_{L_{\dot\alpha}}$ seem to be involved. The numerical simulation shows that the phugoid damping varies substantially only with the derivatives C_{D_u}, C_{m_u}, C_{m_α}, and C_{m_q}.

From Eq. (2)

$$\frac{\partial(2\zeta_p\omega_p)}{\partial X_u} = \frac{g\sin\Theta_1 M_{\dot\alpha} - M_\alpha U_1 + M_q Z_\alpha}{M_\alpha U_1 - M_q Z_\alpha}$$

$$= -1 + \frac{g\sin\Theta_1 M_{\dot\alpha}}{M_\alpha U_1 - M_q Z_\alpha}$$

$$\approx -1$$

because in practice the second term is much smaller than one. From the definition of X_u (Ref. 1), it follows that $2\zeta_p\omega_p$ increases as C_{D_u} increases. Figure 1 shows significant change for aircraft B in flight condition 2.

$$\frac{\partial(2\zeta_p\omega_p)}{\partial M_u} = \frac{U_1(X_\alpha - g)}{M_\alpha U_1 - Z_\alpha M_q} - \frac{g Z_\alpha [U_1(M_{\dot\alpha} + M_q) + Z_\alpha]}{(M_\alpha U_1 - Z_\alpha M_q)^2} \quad (5)$$

The quantity on the right-hand side is sometimes positive and sometimes negative. The numerical simulation indicates that the phugoid damping remains almost invariant with changes in M_u except when M_u approaches the critical value $M_u = (M_\alpha Z_u)/Z_\alpha$. At this value of M_u, $\omega_p = 0$, and the term $2\zeta_p\omega_p$ abruptly becomes zero. When M_u is less than this critical value, there are two real roots to the phugoid.

The numerical simulation shows that $2\zeta_p\omega_p$ is not disturbed by variations in C_{m_α} except at a critical value of C_{m_α} when it behaves violently by abruptly changing its slope to $\pm\infty$. It may be inferred from Eq. (2) that this behavior is caused by the phugoid frequency, which becomes zero at $M_\alpha = (M_u Z_\alpha)/Z_u$ and becomes infinite when $M_\alpha = (M_q Z_\alpha)/U_1$.

Figure 1 shows that when C_{m_q} becomes more and more negative $2\zeta_p\omega_p$ increases in magnitude. The increase is substantial in some cases and mild in others. Figure 1 shows the variation for aircraft E in flight condition 1.

Conclusion

The parametric study undertaken in this paper shows that in the range of interest the frequency and the damping depend only on the derivatives C_{D_u}, C_{m_u}, C_{m_α}, and on C_{m_q}. The speed damping derivative C_{D_u} has no effect on the frequency. The damping increases with increase in C_{D_u}. Phugoid damping is invariant with change in C_{m_u}. When $M_u = (M_\alpha Z_u)/Z_\alpha$, the phugoid frequency vanishes. For M_u less than this critical value, the phugoid mode splits into two first-order roots, with one representing tuck under. Above the critical value, increase of C_{m_u} leads to increase in ω_p. The phugoid damping is invariant with change in C_{m_α}. For large negative values of C_{m_α}, ω_p remains invariant. When $M_\alpha = (M_u Z_\alpha)/Z_u$, the phugoid frequency vanishes. When $M_\alpha = (M_q Z_\alpha / U_1)$, the phugoid frequency becomes infinite. Increase in $|C_{m_q}|$ results in decrease in ω_p (for negative values of C_{m_q}), and increase in $|C_{m_q}|$ results in increase in $2\zeta_p\omega_p$ (for negative values of C_{m_q}). The change is substantial in some cases and mild in others.

Acknowledgment

The author is grateful to the Aeronautics Research and Development Board, New Delhi, India, for providing financial support for this research.

References

[1] Roskam, J., "Airplane Flight Dynamics and Automatic Flight Controls," DAR Corp. Pt. I, Lawrence, KS, 1998.

[2] Kamesh, S., and Pradeep, S., "The Phugoid Approximation Revisited," *Journal of Aircraft,* Vol. 36, No. 2, 1999, pp. 465–467.

[3] Pradeep, S., "A Century of Phugoid Approximations," *Aircraft Design*, Vol. 1, No. 2, Elsevier, Oxford, England, UK, 1998, pp. 89–104.

[4] Pradeep, S., "A Note on the Aft C. G. Location," AIAA Paper 2000-4114, Aug. 2000.

[5] Pradeep, S., and Kamesh, S., "Does the Phugoid Frequency Depend on Speed?" *Journal of Guidance, Control, and Dynamics,* Vol. 22, No. 2, 1999, pp. 372, 373.

Wave Drag Estimation for Use with Panel Codes

N. Petruzzelli* and A. J. Keane†
University of Southampton, Highfield, Southampton, England SO17 1BJ, United Kingdom

I. Introduction

FOR transonic wing designs one of the most important elements in the analysis of aerodynamic performance is the evaluation of wave drag. A common technique for estimating the wave drag of a wing consists in summing the contributions at spanwise sections over the wing. The contribution at each section may be evaluated using methods derived from an exact two-dimensional analysis involving the flow conditions just upstream of the shock wave.[1,2] For each section of the wing, the equivalent two-dimensional flow conditions are then evaluated from the three-dimensional flow conditions using simple sweep theory. The major drawback of such a method is the need for data coming from the three-dimensional flow state around the wing through experimental measurements or full three-dimensional compressible flow state calculations. Such an approach turns out to be not very useful in the context of preliminary concept design, where expensive three-dimensional compressible flow evaluations are to be avoided, where possible, during design optimization. Thus, to reduce the computational cost of wing wave drag evaluation in preliminary design, approximate methods that do not require expensive three-dimensional flow state calculations may be adopted.

Received 19 October 2000; revision received 22 February 2001; accepted for publication 27 February 2001.

*Research Fellow, School of Engineering Sciences. Member AIAA.

†Professor of Computational Engineering, School of Engineering Sciences.